Electronic Supplementary Material (ESI) for Journal of Materials Chemistry A.

Electronic Supporting Information

Perylenetetracarboxylic Diimide as a High-Rate Anode for Potassium-Ion Batteries

Yunfei Bai,[a] Wenbin Fu,[b] Wenhao Chen,[a] Zhichun Chen,[a] Xiaojun Pan,*[b] Xiaoxia Lv,[c] Jincai Wu [a] and Xiaobo Pan*[a]

[a]State Key Laboratory of Applied Organic Chemistry, College of Chemistry and Chemical Engineering, Key Laboratory of Nonferrous Metal Chemistry and Resources Utilization of Gansu Province, Lanzhou University, Lanzhou, 730000, China.

[b]School of Physical Science and Technology, Lanzhou University, Lanzhou, 730000, China.

[c]School of Chemistry and Chemical Engineering, Qufu Normal University, Qufu, 273165, China.

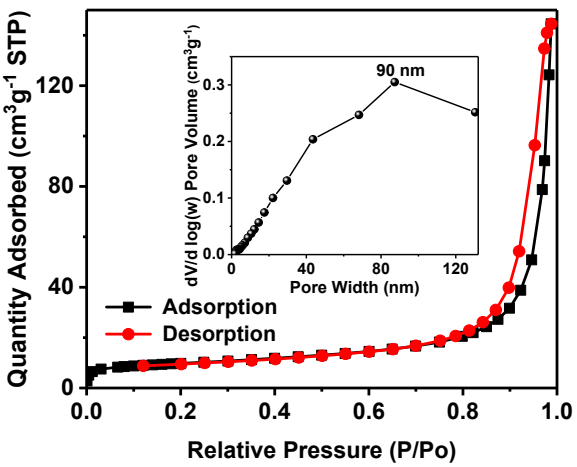

Fig. S1 N_2 adsorption–desorption isotherms of PTCDI and (insert) the pore size distribution.

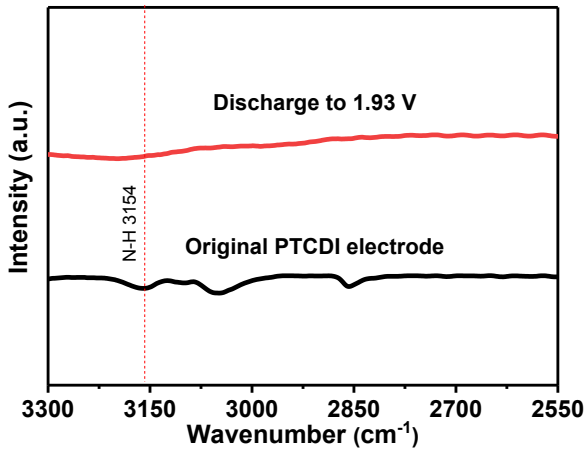

Fig. S2 IR spectra of the original PTCDI electrode and discharging to 1.93 V.

The peak at 3154 cm^{-1} has a significant decrease in the first cathodic scan process, which indicates the removal of H atoms from sp^3 N centers.

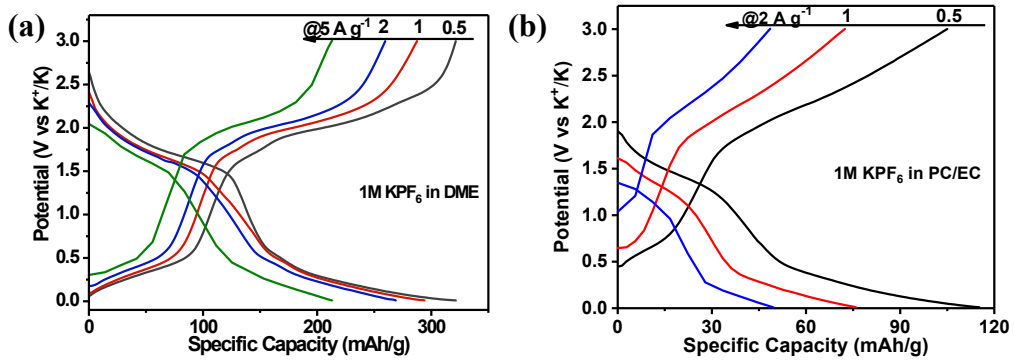

Fig. S3 Galvanostatic charge-discharge curves of PTCDI at current densities of 0.5, 1.0, 2.0, 5.0 A g^{-1} by using 1.0 M KPF_6 in (a) DME and (b) PC/EC (1:1, vol) as the electrolyte.

Table S1 Electrochemical performance of recently reported PIB anode materials

Anodes	Current density (mA g^{-1})	Capacity (mAh g^{-1})	References
Carbonaceous anodes			
PNCM	500	200	1
NCNFs	100	238	2
N-HPC	100	292	3
Inorganic anodes			
T-Nb_2O_5	400	104	4
BiOCl	500	223	5
Fe_3C@PGC-NGF	1000	155	6
Organic anodes			
K_2TP	200	229	7
VK@GNT	100	222	8
ADAPTS	155	128	9
PTCDI	500 and 1000	310 and 290	This work

Table S2 Comparison of the rate performance of PTCDI electrode material in metal ion batteries.

PTCDI electrode	Current density ($mA\ g^{-1}$)	Capacity ($mAh\ g^{-1}$)	References
LIB	100	137	10
	200	133	
	500	130	
	1000	124	
NIB	20	138	11
	300	118	
	600	103	
KIB	500	320	This work
	1000	290	
	2000	246	
	5000	208	

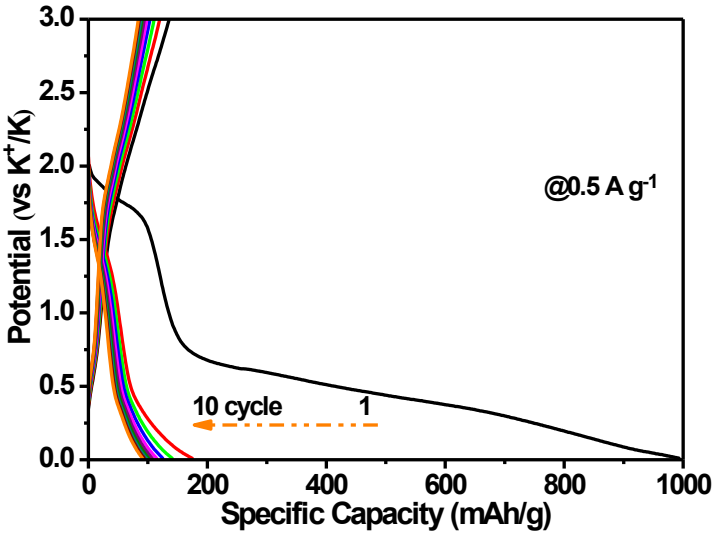

Fig. S4 Representative charge and discharge profiles at a current density of 0.5 A g^{-1} by using 1.0 M KPF_6 in PC/EC (1:1, vol) as the electrolyte.

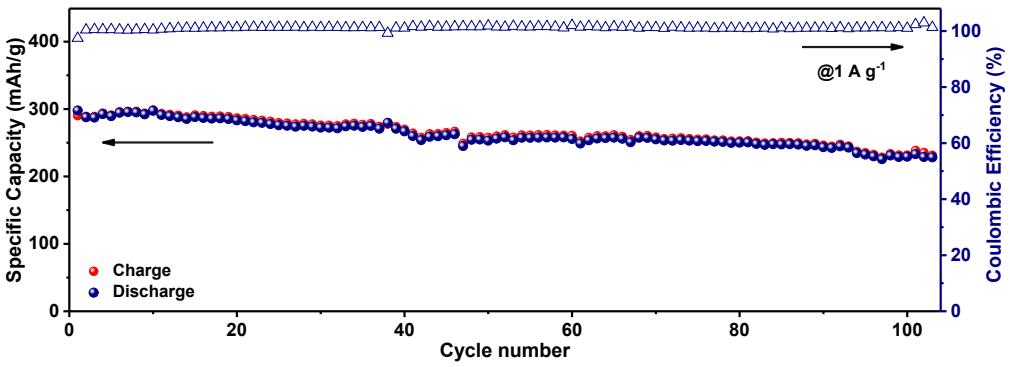

Fig. S5 Capacity stability and columbic efficiency of PTCDI during 100 charge-discharge cycles at 1 A g^{-1} with 1.0 M KPF_6 in DME as electrolyte.

Table S3 Comparison of the electrochemical performance of PIBs with organic anode materials in terms of the specific capacity, the current density, and the cycle number.

Organic anodes	**Capacity/Current density (mAh g^{-1}/mA g^{-1})**	**Cycle number**	**Capacity retention (%)**	**References**
K_2PC	190/44	100	92.6	12
H_2TP	246/50	150	90.6	13
VK@GNT	253.8/100	100	87.5	8
K_2BPDC@GR	200/50	100	85	14
Soft carbon	200/558	50	81.4	15
PTCDI	300 and 218/ 500 and 5000	100 and 320	71.3 and 95.4	This work

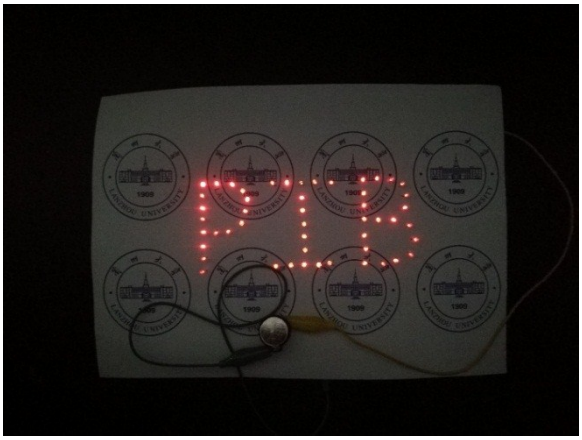

Fig. S6 The full setup optical PIB images of K/PTCDI battery for lighting LED lights

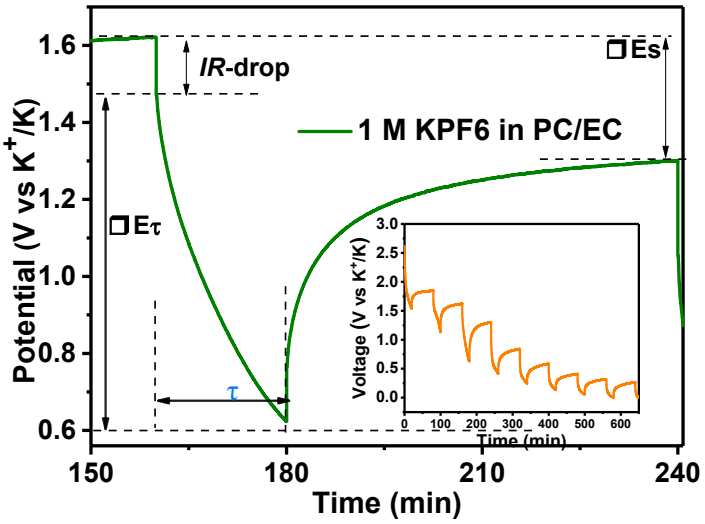

Fig. S7 GITT potential response curve with time for one typical discharge step at 1.6 V of 1 M KPF_6 in PC/EC electrolyte. Inset: GITT profiles of the discharging process selected rest-discharge-rest period.

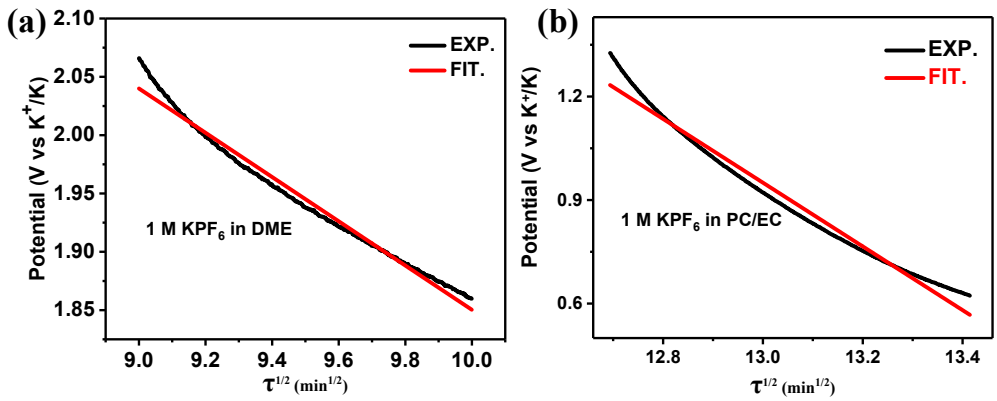

Fig. S8 Voltage variation against $\tau^{1/2}$ at second potassiation process, (a) 1 M KPF_6 in DME and (b) 1 M KPF_6 in PC/EC electrolyte.

GITT measurement was performed by a current pulse at 50 mA g^{-1} for 20 min and rest intervals for 60 min. The K^+ diffusion coefficients in PTCDI were estimated by the Fick's second law using the equation:[16-18]

$$D_{K^+} = \frac{4}{\pi\tau}\left(\frac{m_B V_M}{M_B S}\right)^2\left(\frac{\Delta E_s}{\tau\left(dE_\tau/d\sqrt{\tau}\right)}\right)^2 \quad \left(\tau \ll L^2/D_{K^+}\right) \qquad [1]$$

if the potential *vs.* $\tau^{1/2}$ (τ is pulse current duration time) displays a linear behavior (Fig. S8), equation diffusion can be further simplified as below:

$$D_{K^+} = \frac{4}{\pi\tau}\left(\frac{m_B V_M}{M_B S}\right)^2\left(\frac{\Delta E_s}{\Delta E_\tau}\right)^2 \qquad [2]$$

where m_B is the mass loading (g), V_M molar volume ($cm^3\ mol^{-1}$), the V_M/M_B can be replaced by $1/\rho_B$ (this

parameter corresponding to the pore volume of BET test, $cm^3\ g^{-1}$), S effective area of the electrode (cm^2). Miscellaneous, τ, ΔE_S and $\Delta E\tau$ as depicted in Fig. 4a and S7.

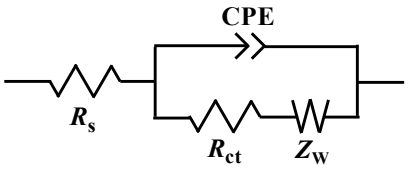

Fig. S9 The equivalent electrical circuit model to fitting EIS spectra. R_s: series resistance, R_{ct}: charge-transfer resistance, CPE: constant phase element, and Z_W: Warburg impedance.

Table S4 Corresponding fitting result of R_s and R_{ct} values for the Nyquist plots

	R_s	R_{ct}
OCV	8.12	93
After 20 cycles	10.12	10.65
After 50 cycles	7.26	3.87

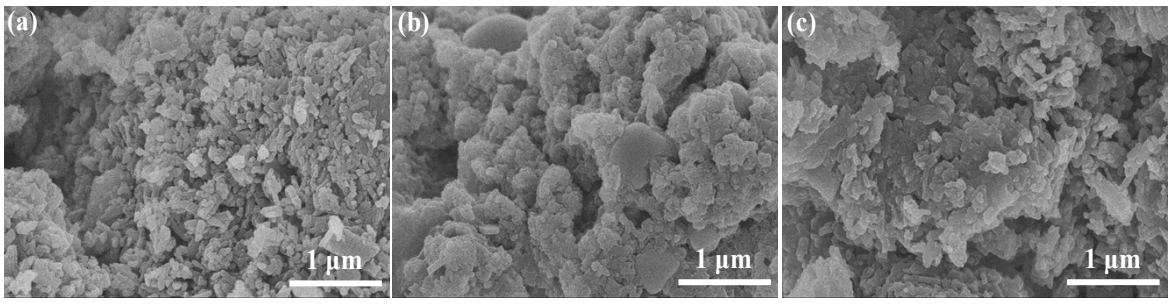

Fig. S10 SEM images of the PTCDI electrodes: (a) fresh electrode, (b) fully potassiation at 0.01 V and (c) fully depotassiation at 3 V.

Cartesian coordinates for the optimized geometries

PTCDI

O	-5.724083	-2.275679	0.000153
O	-5.724087	2.275688	0.000193
N	-5.666313	0.000003	-0.000373
C	-0.735597	-1.249586	0.000006
C	-1.434737	0.000002	-0.000039
C	-0.735587	1.249546	0.000015

C	-1.478329	2.431831	0.000135
C	-2.876838	2.425954	0.000114
C	-3.573019	1.230788	-0.000029
C	-2.865363	-0.000021	-0.000052
C	-3.573039	-1.230826	-0.000034
C	-2.876891	-2.42597	0.000143
C	-1.478349	-2.431824	0.000169
C	-5.055946	-1.253253	-0.000104
C	-5.055855	1.253344	0.000016
H	-6.681511	0.000117	-0.000228
H	-0.977421	3.392298	0.000278
H	-3.4373	3.355038	0.000242
H	-3.437319	-3.355085	0.000283
H	-0.977525	-3.39233	0.000318
C	0.735587	-1.249546	-0.000052
C	0.735597	1.249586	-0.000043
C	1.434737	-0.000003	-0.000001
C	1.47833	-2.431832	-0.000163
C	1.478348	2.431823	-0.0002
C	2.865363	0.000021	0.000013
C	2.876838	-2.425954	-0.000127
H	0.977422	-3.392298	-0.0003
C	2.876891	2.425969	-0.000177
H	0.977524	3.39233	-0.000345
C	3.573019	-1.230788	0.00001
C	3.573039	1.230826	-0.000013
H	3.437301	-3.355038	-0.000235
H	3.437318	3.355085	-0.000326
C	5.055855	-1.253344	0.000018
C	5.055946	1.253253	0.000007
O	5.724088	-2.275687	-0.000081
N	5.666313	-0.000003	0.000402
O	5.724083	2.27568	-0.000004
H	6.681511	-0.000116	0.000351

PTCDI^{2-}

O	-5.750928	-2.278381	0.000209
O	-5.750938	2.278369	0.000185
N	-5.623243	-0.000012	-0.00034
C	-0.716476	-1.246743	0.000026
C	-1.427153	-0.000018	-0.000001
C	-0.716487	1.246722	0.000024
C	-1.482307	2.46314	0.000146
C	-2.850025	2.454312	0.000117
C	-3.578933	1.238951	-0.000059
C	-2.875842	0	-0.000047
C	-3.578939	-1.238942	-0.000054
C	-2.850037	-2.454273	0.000123
C	-1.482312	-2.463162	0.000154
C	-5.023332	-1.265738	-0.000092
C	-5.023302	1.265765	-0.000043
H	-6.636167	0.000049	0.000005
H	-0.967067	3.417482	0.000381
H	-3.419856	3.380006	0.000217
H	-3.419870	-3.379982	0.000212

H	-0.967142	-3.417537	0.000363
C	0.716487	-1.246722	-0.00009
C	0.716476	1.246744	-0.000088
C	1.427153	0.000018	-0.000067
C	1.482306	-2.463140	-0.000201
C	1.482312	2.463162	-0.000197
C	2.875842	0	-0.000019
C	2.850025	-2.454312	-0.000155
H	0.967066	-3.417482	-0.000434
C	2.850038	2.454273	-0.000169
H	0.967142	3.417537	-0.000394
C	3.578933	-1.238951	0.000015
C	3.578939	1.238942	-0.000016
H	3.419855	-3.380006	-0.000233
H	3.41987	3.379982	-0.000259
C	5.023302	-1.265765	0.000059
C	5.023333	1.265738	-0.000016
O	5.750938	-2.278369	-0.000009
N	5.623243	0.000012	0.000387
O	5.750928	2.278381	0.000055
H	6.636167	-0.000049	0.000187

PTCDI^{4-}

O	-5.849946	-2.293446	0.000259
O	-5.849714	2.293452	0.000245
N	-5.659284	0.000066	-0.000559
C	-0.745756	-1.251542	-0.000044
C	-1.458176	0.000042	0.000063
C	-0.745868	1.251492	-0.000115
C	-1.507363	2.445709	-0.000272
C	-2.893856	2.477051	-0.000138
C	-3.639090	1.253489	-0.000014
C	-2.923152	0.000023	0.000059
C	-3.639236	-1.253488	0.000067
C	-2.893759	-2.477060	0.000012
C	-1.507303	-2.445646	-0.00022
C	-5.073884	-1.271054	0.000157
C	-5.073928	1.270954	0.000075
H	-6.672516	0.000101	0.000142
H	-0.979138	3.401287	-0.000519
H	-3.447979	3.414464	-0.000798
H	-3.447747	-3.414524	-0.000779
H	-0.979183	-3.401327	-0.000452
C	0.745868	-1.251492	0.000111
C	0.745755	1.251542	0.000080
C	1.458176	-0.000041	-0.000046
C	1.507362	-2.445708	0.000209
C	1.507303	2.445647	0.000307
C	2.923152	-0.000023	-0.000046
C	2.893856	-2.47705	0.000061
H	0.979137	-3.401287	0.000414
C	2.893759	2.47706	0.000084
H	3.63909	-1.253489	-0.000017
C	3.639236	1.253488	-0.000014
H	3.447979	-3.414464	0.000669

H	3.447747	3.414524	0.000921
C	5.073928	-1.270954	-0.000118
C	5.073884	1.271054	-0.000104
O	5.849713	-2.293452	-0.000359
N	5.659284	-0.000067	0.000548
O	5.849948	2.293445	-0.000238
H	6.672516	-0.000101	-0.000179

PTCDI^{6-}

O	-5.947698	-2.307849	0.044586
O	-5.947865	2.307882	0.044055
N	-5.754124	-0.000031	-0.218138
C	-0.732362	-1.263244	0.018859
C	-1.507792	0.000022	-0.003906
C	-0.732417	1.263186	0.018538
C	-1.52683	2.448432	0.08685
C	-2.921681	2.48426	0.079251
C	-3.710581	1.270194	-0.00406
C	-2.930002	-0.000023	-0.017536
C	-3.710539	-1.270278	-0.00381
C	-2.921627	-2.48429	0.079944
C	-1.526715	-2.448396	0.0876
C	-5.120861	-1.281112	-0.030154
C	-5.120878	1.280906	-0.030325
H	-6.703602	0.000052	0.159292
H	-1.006714	3.414543	0.173812
H	-3.455153	3.441807	0.138814
H	-3.454974	-3.441869	0.139824
H	-1.006622	-3.414521	0.174991
C	0.732406	-1.263137	-0.018606
C	0.732368	1.263292	-0.018567
C	1.507791	0.000015	0.004016
C	1.526783	-2.448376	-0.087424
C	1.526756	2.448449	-0.086848
C	2.93	0.000026	0.017624
C	2.921633	-2.484234	-0.079898
H	1.006621	-3.414424	-0.174827
C	2.921669	2.484312	-0.079163
H	1.006706	3.414636	-0.173808
C	3.710553	-1.270206	0.003816
C	3.710565	1.270266	0.004198
H	3.455089	-3.441757	-0.139999
H	3.45503	3.441915	-0.138546
C	5.120852	-1.280951	0.030008
C	5.120887	1.281074	0.030493
O	5.947816	-2.307906	-0.044882
N	5.754151	-0.000073	0.218055
O	5.947746	2.307787	-0.044364
H	6.703568	-0.000088	-0.159533

References for Supplementary Information

1 Y. Xie, Y. Chen, L. Liu, P. Tao, M. Fan, N. Xu, X. Shen and C. Yan, *Adv. Mater.*, 2017, **29**, 1702268.

2 Y. Xu, C. Zhang, M. Zhou, Q. Fu, C. Zhao, M. Wu and Y. Lei, *Nat. Commun.*, 2018, **9**, 1720.

3 X. Zhou, L. Chen, W. Zhang, J. Wang, Z. Liu, S. Zeng, R. Xu, Y. Wu, S. Ye, Y. Feng, X. Cheng, Z. Peng, X. Li and Y. Yu, *Nano Lett.*, 2019, **19**, 4965-4973.
4 N. Li, F. Zhang and Y. Tang, *J. Mater. Chem. A*, 2018, **6**, 17889-17895.
5 W. Li, Y. Xu, Y. Dong, Y. Wu, C. Zhang, M. Zhou, Q. Fu, M. Wu and Y. Lei, *Chem. Commun.*, 2019, **55**, 6507-6510.
6 K. Han, Z. Liu, P. Li, Q. Yu, W. Wang, C.-Y. Lao, D. He, W. Zhao, G. Suo, H. Guo, L. Song, M. Qin and X. Qu, *Energy Storage Mater.*, 2019, DOI: https://doi.org/10.1016/j.ensm.2019.01.016.
7 K. Lei, F. Li, C. Mu, J. Wang, Q. Zhao, C. Chen and J. Chen, *Energy Environ. Sci.*, 2017, **10**, 552-557.
8 Q. Xue, D. Li, Y. Huang, X. Zhang, Y. Ye, E. Fan, L. Li, F. Wu and R. Chen, *J. Mater. Chem. A*, 2018, **6**, 12559-12564.
9 Y. Liang, C. Luo, F. Wang, S. Hou, S.-C. Liou, T. Qing, Q. Li, J. Zheng, C. Cui and C. Wang, *Adv. Energy Mater.*, 2019, **9**, 1802986.
10 D. Wu, F. Jing, X. Xi, L. Ma, D. Lu, P. Yang and R. Liu, *J. Colloid Interface Sci.*, 2019, **538**, 597-604.
11 W. Deng, Y. Shen, J. Qian, Y. Cao and H. Yang, *ACS Appl. Mater. Interfaces*, 2015, **7**, 21095-21099.
12 Q. Deng, J. Pei, C. Fan, J. Ma, B. Cao, C. Li, Y. Jin, L. Wang and J. Li, *Nano Energy*, 2017, **33**, 350-355.
13 C. Wang, W. Tang, Z. Yao, Y. Chen, J. Pei and C. Fan, *Org. Electron.*, 2018, **62**, 536-541.
14 C. Li, Q. Deng, H. Tan, C. Wang, C. Fan, J. Pei, B. Cao, Z. Wang and J. Li, *ACS Appl. Mater. Interfaces*, 2017, **9**, 27414-27420.
15 Z. Jian, W. Luo and X. Ji, *J. Am. Chem. Soc.*, 2015, **137**, 11566-11569.
16 W. Weppner and R. A. Huggins, *J. Solid State Chem.*, 1977, **22**, 297-308.
17 C. Bommier, T. W. Surta, M. Dolgos and X. Ji, *Nano Lett.*, 2015, **15**, 5888-5892.
18 Z. Jian, Z. Xing, C. Bommier, Z. Li and X. Ji, *Adv. Energy Mater.*, 2016, **6**, 1501874.